

RESEARCH ARTICLE SUMMARY

HUMAN DEVELOPMENT

An interactive three-dimensional digital atlas and quantitative database of human development

Bernadette S. de Bakker,* Kees H. de Jong, Jaco Hagoort, Karel de Bree, Clara T. Besselink, Froukje E. C. de Kanter, Tyas Veldhuis, Babette Bais, Reggie Schildmeijer, Jan M. Ruijter, Roelof-Jan Oostra, Vincent M. Christoffels, Antoon F. M. Moorman*

INTRODUCTION: The basic human body plan, the arrangement of organs in the body, is laid down during embryonic development. Insight into the formation of this plan informs researchers and clinicians about normal development versus the development of congenital malformations, the latter of which have an incidence of 3% in the human population and cause up to one-quarter of all neonatal deaths. Despite modern technologies such as three-dimensional imaging, the intricate morphogenesis of the developing human body is difficult to understand. Textbooks on human development are often based on the works of early embryologists, some published more than 100 years ago. Because of the limited availability of human embryonic specimens, it is difficult or impossible to independently verify the information carried

in these textbooks, or even to assess whether this information is derived from studies on human or animal models.

RATIONALE: Current imaging and computer technology make it possible to reconstruct human development with sufficient resolution to visualize organ development. Stained histological sections (mainly from the Carnegie Collection of human embryos) were digitized, tissues and organs were identified, and knowledge-driven modeling was applied to correct imperfections in the three-dimensional reconstructions.

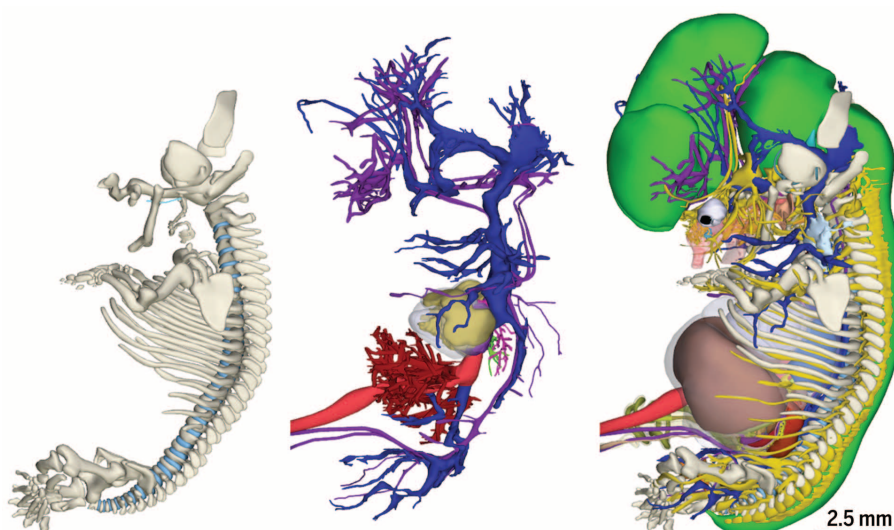
RESULTS: We created a digital atlas with 14 interactive three-dimensional models of human embryology and a database encompassing 34

embryos spanning the first 2 months of human development. Approximately 15,000 histological sections from the Carnegie Collection were analyzed by trained biomedical students under expert supervision, and up to 150 organs and structures were identified and digitally labeled in each section. The labeled structures were then spatially reconstructed in such a way that the relation between the reconstruction and the original images was preserved. We tested the reproducibility of the manual tracing of the different organs and found that the variability in volumes of segmented structures ranged from 0.3% to 2% between students for simple and complex structures, respectively. The 3D models, supplemented by an object tree with structures

named in accordance with the international standard of embryonic terminology, the *Terminologia Embryologica*, are presented as interactive 3D-PDFs, which facilitates exploration of the complex

relations between the different organs and allows researchers to develop an independent view of their spatial relations. The 3D reconstructions enable the measurement of the growth of the individual organs and structures, the assessment of the changing position of organs relative to vertebral segments during development, and the verification of remaining ambiguities in the descriptions of the development of organs.

CONCLUSION: The morphology presented in this atlas is directly connected to the original sections of the embryos in the Carnegie Collection—a connection that was in danger of being lost, with present-day textbook morphology becoming increasingly schematic and deviating from the original substrate. A number of detailed analyses of the development of the kidney, pharyngeal arch cartilages, and notochord show that the current descriptions of the development of these organs are based on comparative animal models rather than on factual observations in human specimens. These examples demonstrate the scientific value of the atlas. This atlas will therefore serve as an educational and reference resource for students, clinicians, and scientists interested in human development and development-related congenital diseases. The 3D-PDFs of the reconstructions, as well as original and labeled images, are freely available (<http://3datlasofhumanembryology.com>). ■



Lateral views of a model of a 7.5-week-old human embryo (16 mm). Left: Skeletal system. Center: Cardiovascular system with transparent heart muscle. Venous system is shown in blue, arterial system in purple, liver vessels in red, and umbilical vein in pink. Right: Reconstructed organs, except skin. Note, for example, the neural tube in green and the nerves in yellow.

The list of author affiliations is available in the full article online.
*Corresponding author. Email: b.s.debakker@amc.uva.nl
(B.S.d.B.); a.f.moorman@amc.uva.nl (A.F.M.M.)
Cite this article as B. S. de Bakker et al., *Science* **354**, aag053 (2016). DOI: 10.1126/science.aag053

RESEARCH ARTICLE

HUMAN DEVELOPMENT

An interactive three-dimensional digital atlas and quantitative database of human development

Bernadette S. de Bakker,* Kees H. de Jong, Jaco Hagoort, Karel de Bree, Clara T. Besselink, Froukje E. C. de Kanter, Tyas Veldhuis, Babette Bais, Reggie Schildmeijer, Jan M. Ruijter, Roelof-Jan Oostra, Vincent M. Christoffels, Antoon F. M. Moorman*

Current knowledge about human development is based on the description of a limited number of embryonic specimens published in original articles and textbooks, often more than 100 years ago. It is exceedingly difficult to verify this knowledge, given the restricted availability of human embryos. We created a three-dimensional digital atlas and database spanning the first 2 months of human development, based on analysis of nearly 15,000 histological sections of the renowned Carnegie Collection of human embryonic specimens. We identified and labeled up to 150 organs and structures per specimen and made three-dimensional models to quantify growth, establish changes in the position of organs, and clarify current ambiguities. The atlas provides an educational and reference resource for studies on early human development, growth, and congenital malformations.

The basic human body plan is laid down during embryonic development. Insight into the formation of this plan has been shown to provide rational explanations for the relative positions of organs in the adult, as well as for the origin of congenital malformations. Congenital defects have an incidence of 3% in the human population (1) and cause up to one-quarter of all neonatal deaths (2). Knowledge of normal human development is therefore of great clinical interest, particularly for pediatricians and clinical geneticists. Despite modern approaches such as three-dimensional (3D) reconstruction, it remains difficult to map the intricate morphogenesis of the developing human body. Current textbooks (3–6) on human development are usually based on the articles and textbooks of various stellar embryologists (7–24), often published more than 100 years ago. However, it is almost impossible to independently verify the information presented in these textbooks, or even to assess whether this information is derived from studies on human or animal material.

By visualizing development, normal embryogenesis and even malformations can be better understood. In this study, we provide an atlas and database spanning the entire embryonic period of human development, covering early organogenesis based on human embryonic specimens from the Carnegie Collection (table S1).

The Carnegie Collection consists principally of serially sectioned normal human embryos in the first 8 weeks of development. It was started by the Carnegie Institution of Washington's Department of Embryology in 1914.

Our interactive atlas allows the user to directly link the annotated organs in the 3D reconstructions with the underlying histological sections of the Carnegie Collection, thereby enabling independent verification and further analyses. The atlas identifies differential growth and the changing relative positions of organs and structures during the first 8 weeks of human development in a quantitative fashion. Initial analyses provide new insights into these relationships.

Data generation and reconstruction pipeline

The degree of detail required for 3D reconstructions of distinct organ systems in early development is currently impossible to obtain with noninvasive techniques such as magnetic resonance imaging (25, 26). Moreover, with a few exceptions, the scarcity of human embryos does not permit tissue identification based on specific immunostaining of the individual organs. Because of these limitations, we chose to analyze histological sections from the Carnegie Collection, with manual identification and labeling of every organ and structure, followed by knowledge-driven modeling to prevent loss of essential detail.

A flowchart of the methods used to generate the 3D reconstructions and morphometric contents of the database is presented in Fig. 1. We imaged and analyzed 17 embryonic stages,

with two embryos per stage, spanning the first 2 months of development, which corresponds to Carnegie stages (CS) 7 to 23 (15 to 60 days of development; table S1). We analyzed stages CS7 (15 to 17 days of development), CS8 (17 to 19 days), CS9 (19 to 21 days), CS10 (21 to 23 days), CS11 (23 to 26 days), CS12 (26 to 30 days), CS13 (28 to 32 days), CS14 (31 to 35 days), CS15 (35 to 38 days), CS16 (37 to 42 days), CS17 (42 to 44 days), CS18 (44 to 48 days), CS19 (48 to 51 days), CS20 (51 to 53 days), CS21 (53 to 54 days), CS22 (54 to 58 days), and CS23 (56 to 60 days). Although analysis of two specimens per stage is insufficient to estimate variance in development, the extensive series of embryonic stages allows generalization of continuous patterns of growth. Images were acquired from about 15,000 histologically stained sections, and up to 150 organs and structures per specimen were manually segmented and spatially reconstructed. Structures were identified on the basis of anatomical and histological characteristics and named in accordance with the international standard of embryonic terminology, the *Terminologia Embryologica* (27). The morphological reconstructions were prepared with Amira and Blender software (see supplementary materials). The 3D reconstructions were made in such a way that the original sections can be placed within the reconstruction, permitting independent verification of the identification of organs.

The variability of the organ volumes measured by different observers ranged from 0.3% to 2% for simple and complex structures (fig. S1). A smooth and easily recognizable organ, such as the otic vesicle, is considered a simple structure, whereas a small and tangled structure, such as the mesonephros and mesonephric duct, consisting of different types of tissue, is termed a complex structure. This small interobserver variation underscores the reproducibility of the segmentation and reconstruction process.

Because organ morphology gradually and consistently changed both qualitatively and quantitatively in the embryonic series studied, we conclude that no grossly abnormal embryos were included in the study and that the staging of the embryos was accurate.

The applied reconstruction protocol has dual outputs: (i) a series of 14 3D reconstructions that covers the entire embryonic period in an interactive format that can be viewed on different computer types and smartphones (3D-PDF format), and (ii) a set of tables and figures that provides quantitative information about the growth of the distinct structures, as well as demonstrates the changing position of structures relative to the vertebral column. The reconstructions provide spatial information, including observations about the complex and changing relationships between different structures in the developing embryo (supplementary 3D-PDFs). The information in the tables and figures allows interpretation of organ growth relative to the growth of the embryo (data S1) and enables the choice of reference points for analysis of specific organs (data S2).

Department of Anatomy, Embryology and Physiology, Academic Medical Center, Amsterdam, Netherlands.
*Corresponding author. Email: b.s.debakker@amc.uva.nl (B.S.D.B.); a.f.moorman@amc.uva.nl (A.F.M.M.)

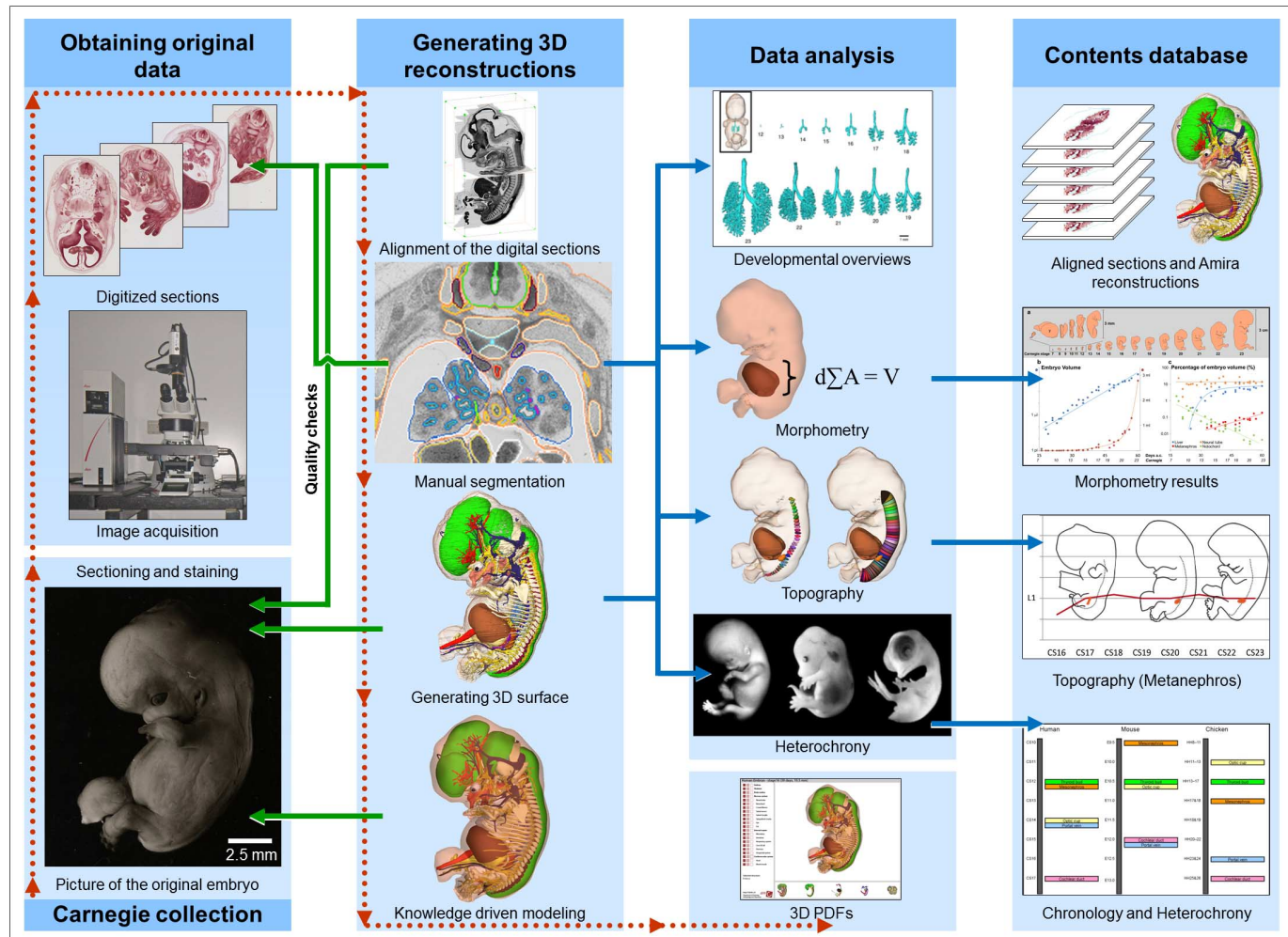


Fig. 1. Flowchart of three-dimensional reconstruction, model generation, and data analysis. Histologically stained sections of the embryos from the Carnegie Collection were imaged, aligned, and segmented. Three-dimensional models were created in the 3D reconstruction package Amira; surfaces were smoothed, without loss of essential details, by knowledge-driven modeling in Blender. The resulting 3D models were then incorporated into interactive 3D-PDF files. Data analysis was performed on the seg-

mented sections and the 3D models. The resource database contains the aligned images, the segmented Amira models, the interactive 3D-PDFs, and tables and graphs of the quantitative, topographic, and developmental data of all structures in every specimen. Green arrows indicate quality checks; red and blue arrows indicate the flow of data toward the contents of the resource database. Stage 20 specimen 462 was used to illustrate this flowchart.

Interactive three-dimensional models of early human development

The supplementary 3D-PDFs comprise 14 interactive 3D-PDF files, covering the first 2 months of human development, and illustrate the complex morphological changes that occur during development. With the interactive version, it is possible to focus on a specific organ, or on the system related to the organ of interest. An example of a 3D model of a CS20 embryo (51 to 53 days) is shown in Fig. 2. This view shows the nervous system in relation to the developing skeleton. Note that the vertebral arches are not yet closed and that the vertebral column and the spinal cord are still of equal length; the relative ascent of the latter has yet to occur.

To illustrate the scientific potential of these models, we analyzed the development of the vasculature in detail, summarized the results in schematics (Fig. 3, table S2, and fig. S2, A to O),

and tabulated notable differences from the literature (3–6, 9, 28–30) (table S3). Some conspicuous differences from the literature are in the connections of the umbilical arteries with the aorta, the origin of the intestinal arteries, the sprouting of the pulmonary arteries, the origin of the external carotid artery, and the absence of the fifth pharyngeal arch artery in all embryos (table S3). It is difficult to trace when and why the descriptions in textbooks started to deviate from reality in the human embryo, because it is impossible to recover the original sources of these texts.

The organization of embryonic growth

The growth rate of the embryo, as derived from interpolation of the volumes of the series of embryos, is remarkably constant in the first 2 months of development. During this period the embryo grows exponentially; its volume increases 25% per day and reaches a volume

of 2790 mm^3 at 60 days of development, or CS23 (Fig. 4, A and B). Nonetheless, there are substantial differences among the growth rates of different organs, which lead to differential relative growth between organs and between developmental phases (Fig. 4C and data S1). The liver initially grows substantially faster than does the entire embryo, but at stage 15/16 its growth rate tapers off to match the overall growth rate (Fig. 4C, blue line). The notochord shows an exponential decline in relative volume, whereas the metanephros grows faster than the total embryo (Fig. 4C, green and red line, respectively). The neural tube (minus neural canal) and its derivatives, in contrast, grow at a rate similar to that of the entire embryo throughout the period analyzed and thus show a constant relative volume of 10% (Fig. 4C, yellow line).

We tabulated the first appearance, and sometimes disappearance, of the different organs and

Fig. 2. Three-dimensional model of a stage 20 human embryo (specimen 462 of the Carnegie Collection, 7.5 weeks of development).

(A) Lateral view of the original embryo before sectioning. (B) Lateral view of all reconstructed organs and structures, except for the skin.

(C) Three-dimensional view of the reconstructed embryo highlighting the skeleton and neural tube. The sagittal plane cuts through the digitized image stack. (D) Cranial view on the transverse section from (C) through the shoulder region.

(E) A detail of a transverse section through the lungs, as presented in Amira. Note the colored outline of each annotated structure. The neural tube is represented in green, the skeleton in off-white; the transparent body cavities enable inspection of the liver (brown). Scale bars, 2.5 mm [(A) to (C)], 1 mm [(D) and (E)].

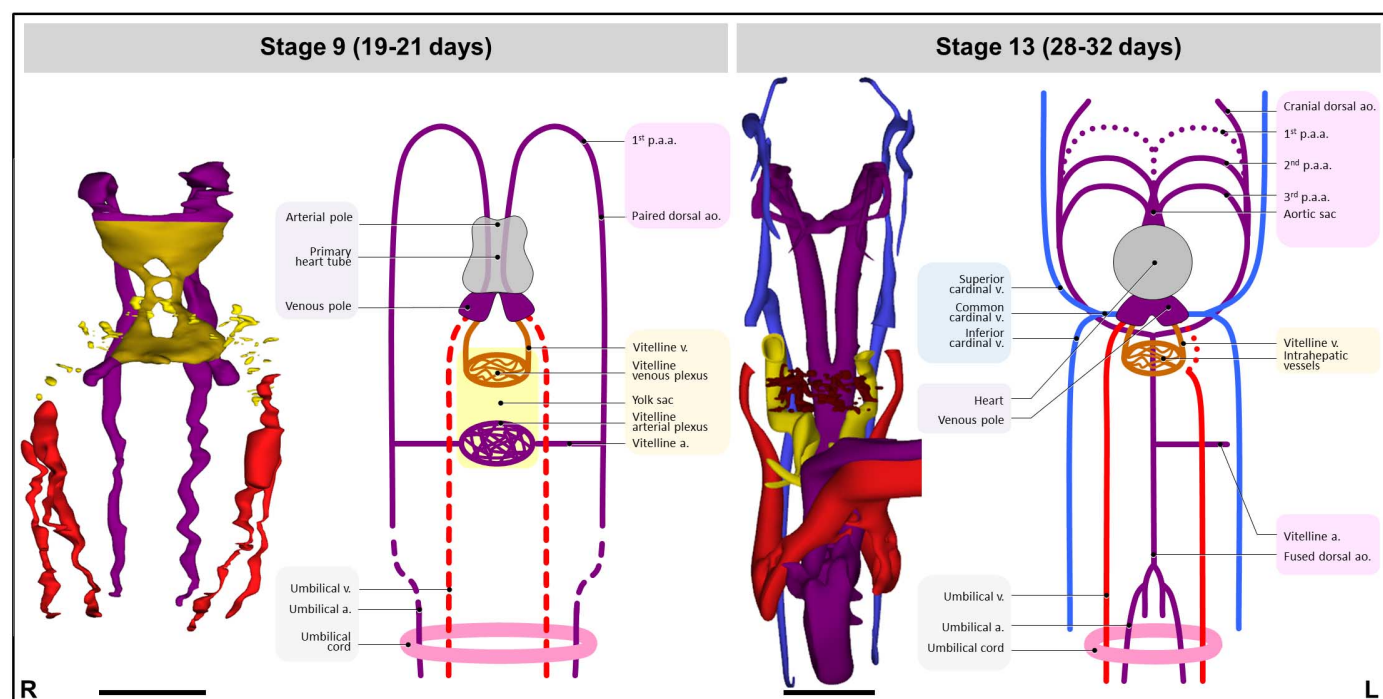
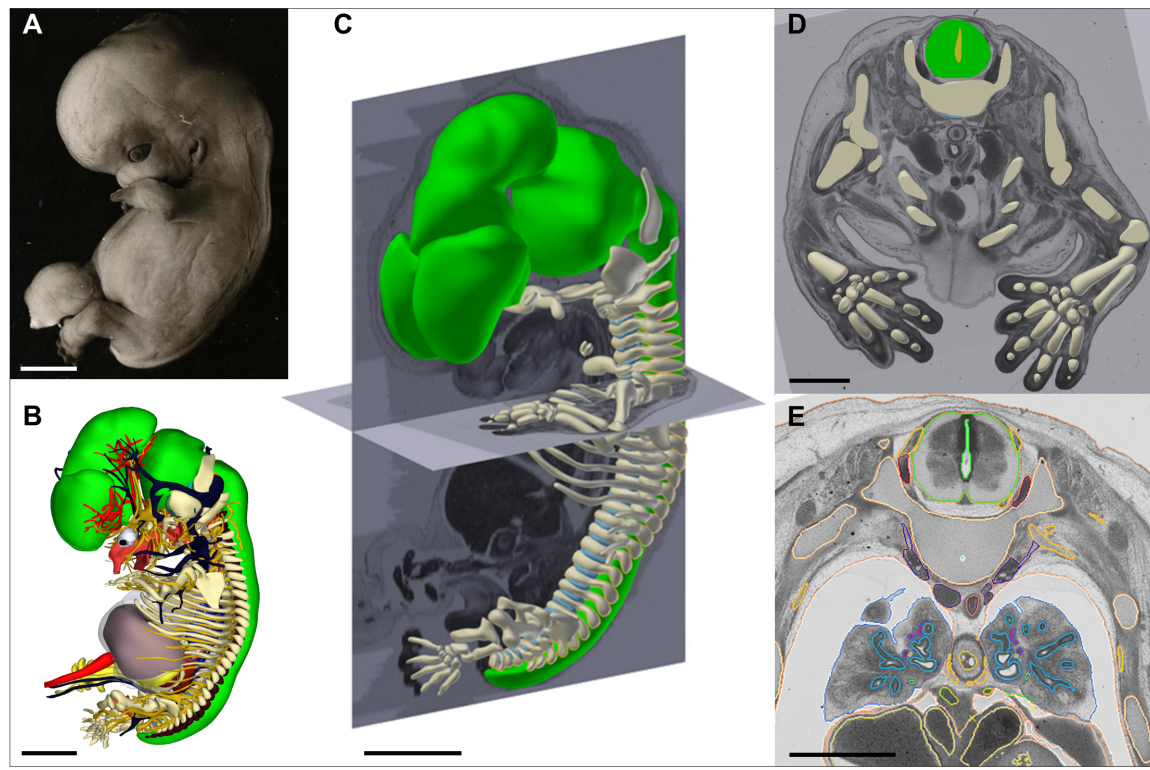


Fig. 3. Development of the vascular system. The developing vascular system is presented in a Carnegie stage 9 embryo (19 to 21 days; left) and a stage 13 embryo (28 to 32 days; right). Dashed lines represent developing vessels; dotted lines represent regressing vessels. See fig. S2, A to O, for a complete schematic overview of the developing vascular system between stage 9 (19 to 21 days) and stage 23 (56 to 60 days). Changes in the vascular system are summarized per stage in tables S2 and S3. Abbreviations: a., artery; ao., aorta; p.a.a., pharyngeal arch arteries; v., vein. Scale bars, 250 μ m (stage 9), 500 μ m (stage 13).

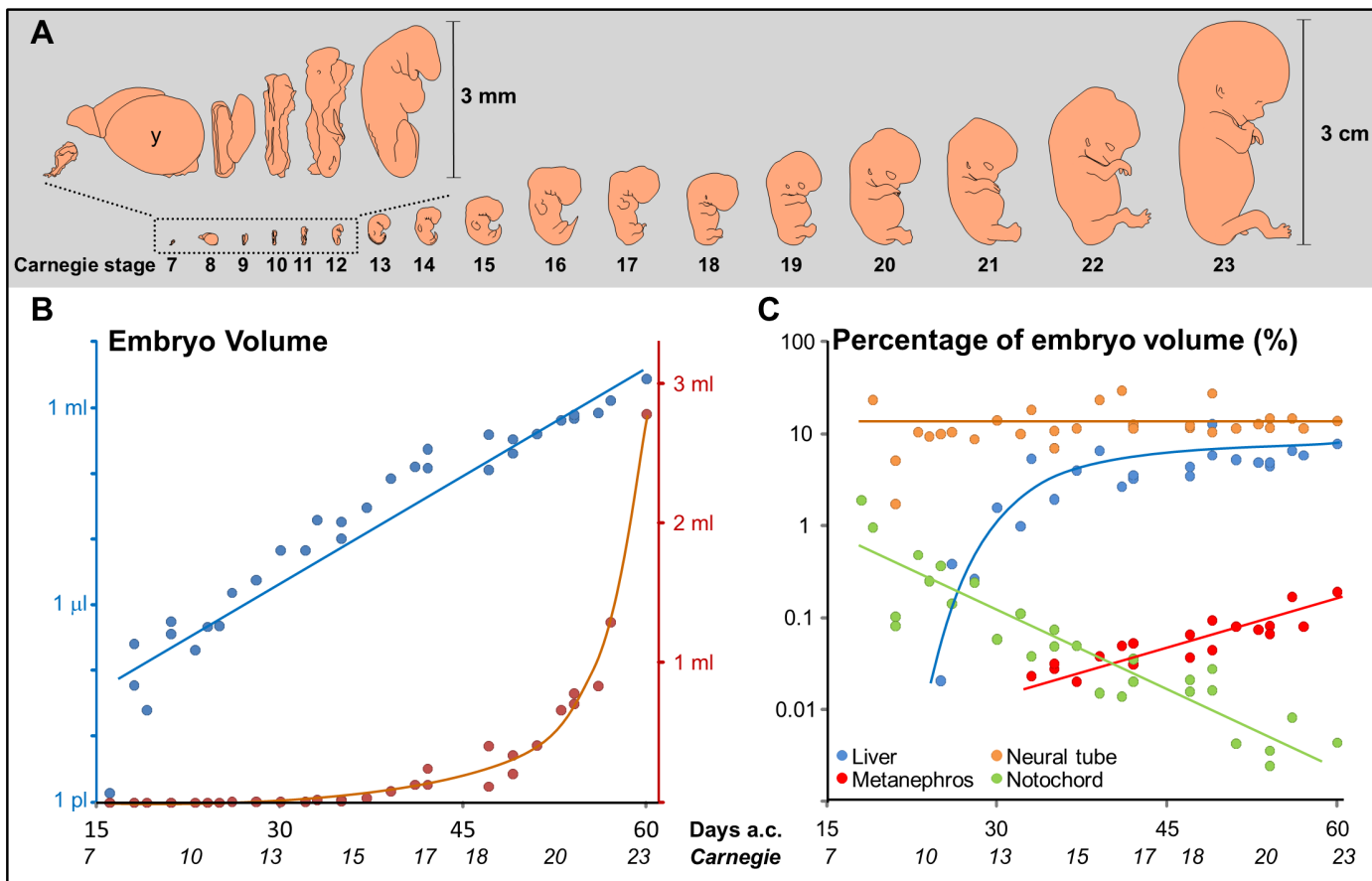


Fig. 4. Growth of the human embryo during the first 2 months of development. (A) Length of the embryo between Carnegie stages 7 and 23. Stages 7 to 12 are enlarged. Note the large round yolk sac (y) in stage 8. Drawings (left to right) are of specimens 8752, 8671, H712, 6330, 6784, 8505A, 0836, 8314, 3512, 6517, 8521, 8524, 2114, 462, 7258, 895, and 9226. (B) Increase in body volume with respect to days after conception (days a.c.) and Carnegie stages (x axis). Embryo volumes are plotted on a logarithmic scale (left y axis; blue dots) and on a linear scale (right y axis; red dots). The linear relation between $\log(\text{volume})$ and days of development indicates a

constant growth rate of the embryos in this development period. (C) Relative volume of organs as percentage of embryonic volume (y axis) with respect to days after conception and Carnegie stages (x axis). Neural tube (not including the neural canal), liver, metanephros, and notochord are shown as examples (see data S1 for other organs). The neural tube accounts for a constant relative volume of $\sim 10\%$ of the total volume, whereas the relative volume of the liver first increases, after which it also reaches a steady relative volume of 8% . The relative volume of the notochord decreases exponentially, whereas the relative volume of the metanephros increases exponentially after its first appearance.

structures within the human embryo for each stage, and compared the findings with the corresponding data for mouse and chicken embryos (fig. S3 and data S3). This analysis is of particular importance in teratological studies that apply data from experimental animals to the human situation. The order of appearance of the distinct organs in these species agrees largely with the order reported by Butler and Juurlink (31), who based their staging exclusively on the exterior characteristics of the complete embryo. However, we found a consistent difference of one to two stage equivalents when comparing matched mouse and human or chicken developmental stages (fig. S3 and data S3). Thus, our data show that mouse embryonic day 9.5 (E9.5) corresponds to CS12 rather than CS10, and so on. However, we also found different timing of the appearance of some internal organs, such as the choroid plexus, which is first recognizable in mouse stage E11.0 but only five equivalent stages later in human (CS18) and chicken (HH27 to 28)

(data S3). Similarly, the regression of the stalk of the pharyngeal hypophysis is completed six stages earlier in mouse (E12.0) than in human (CS21) and chicken (HH33 to 34) (data S3). The adrenal gland, in contrast, starts to develop in the same stage in human (CS18) and mouse (E13.5) embryos, but four equivalent stages later in chicken embryos (HH35) (data S3). In the current literature, the data for the timing of development of structures within the human embryo are anecdotal (32, 33), and textbooks are inconsistent and lack references (3–6, 18, 29, 30, 34). Overall, our tabulated human data are consistent with those presented in the atlas of human development by O'Rahilly and Müller (18).

Changing organ topography

Regional differences in growth and migration of the organs are usually suggested to explain the changes of the position of organs during development (3–6, 18, 35, 36). Perhaps the most cited example is the ascent of the primordial

kidneys (3–6, 34). This ascent, in turn, has led to the notion that fusion of the kidney primordia, prior to their ascent, would account for the horseshoe lesion, the fused middle part allegedly being prevented from ascent by the presence of the midline inferior mesenteric artery, whereas the lateral parts have no impediment to their ascent (3–6). The greatest weakness of these suppositions is the almost total lack of quantitative data about the relative positions of the different structures during development. Our 3D reconstructions permit us to show the position of each individual organ relative to the developing vertebrae (Fig. 5 and data S2). The primordium of the definitive kidney, or metanephros, can be identified already at CS14, but we could first reliably relate its position to the developing vertebrae at CS16 (Fig. 5). The kidney is then positioned within the lumbar region extending from the fourth lumbar vertebra to the first sacral vertebra. Within a few days, it elongates up to the level of the first lumbar vertebra (CS17). Its cranial margin

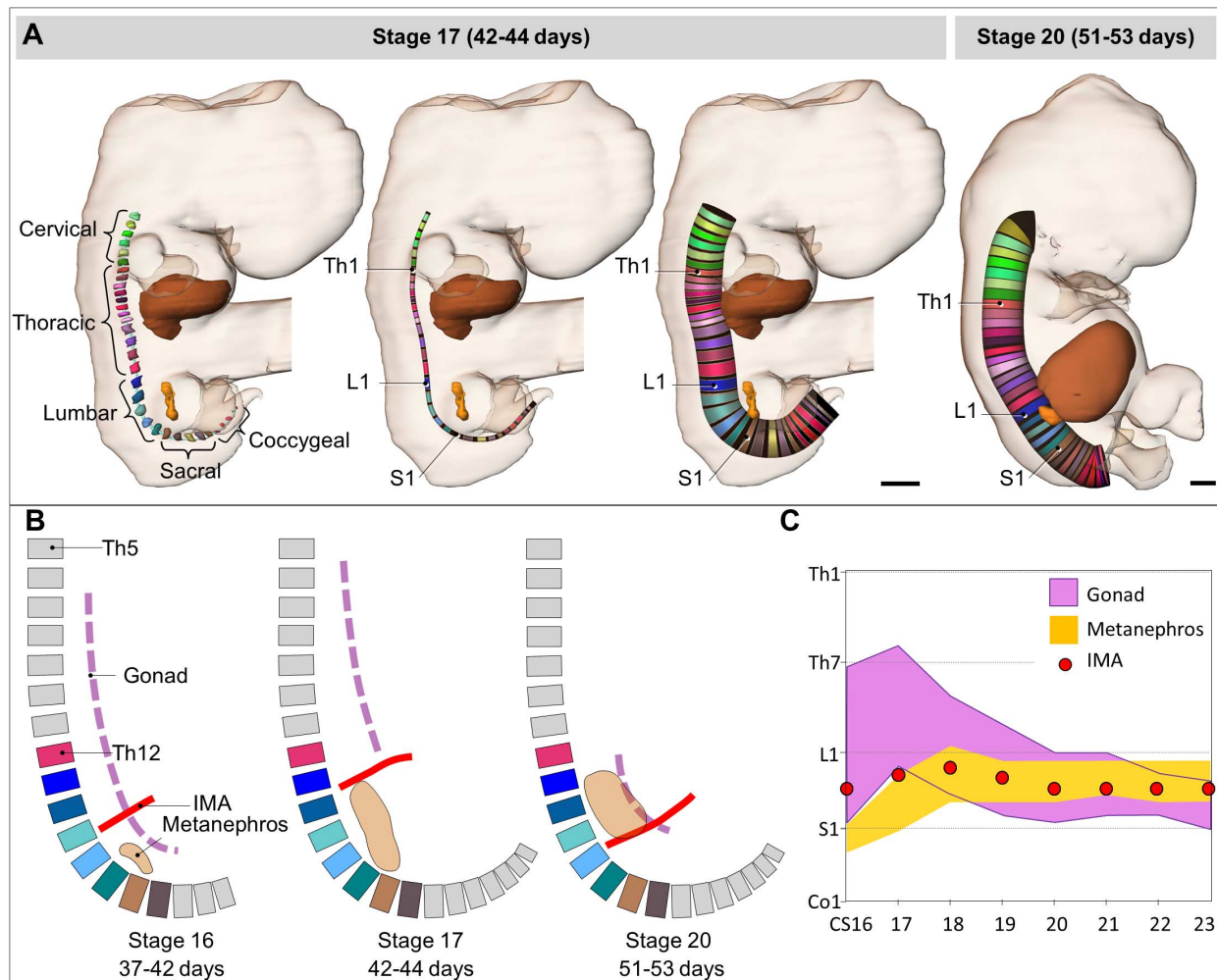


Fig. 5. Assessment of organ position during development. (A) To enable determination of the position of organs, planes perpendicular to the notochord were generated from the intersection of the developing vertebrae with the notochord. Left: Reconstruction of the individually labeled vertebrae and notochord. Center: The notochord was skeletonized to a line and masked with the colors of the vertebrae. Right and far right: The skeletonized notochord was expanded to form a cylinder. Each colored disc corresponds to a vertebra, and the planes of these discs, perpendicular to the notochord, now serve as rulers. The user can increase the diameter of the discs to determine which discs intersect with the organ of interest. The most cranial and caudal intersections of an organ with the planes of the discs then give the position of an organ relative to the vertebrae. Stage 17 (specimen 6521)

and stage 20 (specimen 462), with annotated liver (brown) and kidneys (orange), are illustrated. Note the caudal shift of the liver from stage 17 (C7-Th10) to stage 20 (Th2-S5), whereas the kidneys remain at the same cranial position (L1), in contrast to descriptions in textbooks. (B) Cartoons based on 3D reconstructions. The relation of the metanephros (orange), the gonad (purple), and the inferior mesenteric artery (IMA; red) is indicated in stages 16, 17, and 20. See the text for their positional changes. (C) Margins of the position of the metanephros (orange band), the inferior mesenteric artery (red dots), and the gonads (purple band) during development (x axis) relative to the vertebrae (y axis) (see data S2 for other organs). Th, thoracic; L, lumbar; S, sacral; Co, coccygeal; CS, Carnegie stage. Scale bars in (A), 1 mm.

remains at this “adult” level, whereas during further development its caudal margin “ascends” from the first sacral to the fourth lumbar vertebra, owing to a relatively faster growth of the developing vertebral column. This raises the question of whether such a pattern of growth implies a real ascent of the kidneys during development.

A confounding factor that may have led to the notion of ascent of the kidneys is the hitherto unrecognized substantial difference in growth along the entire length of the aorta, which determines the relative position of the arterial branches (Fig. 5, fig. S2, H to O, and data S2). During development, the branching point of the seventh inter-

segmental artery remains positioned at the level of the seventh cervical vertebra and that of the umbilical arteries at the level of the third to fourth lumbar vertebrae, whereas the relative positions of the three major intestinal arteries change considerably. From CS16 to CS23, the branching point of the celiac trunk and the superior mesenteric artery “descends” from the sixth and seventh thoracic vertebrae, respectively, to the first lumbar vertebra; the inferior mesenteric artery “descends” only slightly from the first to the third lumbar vertebra. As a consequence, the position of this latter artery changes from the cranial border of the kidney at CS17 to

its caudal border from stage 20 onward. Therefore, taking this artery as the point of reference gives the erroneous impression that the kidneys ascend.

Another example is the developing gonads, which are generally assumed to descend during development (4–6, 29). Our data show that this is not the case. During the embryonic period, the caudal margin of the developing gonads remains approximately at the level of the fifth lumbar or first sacral vertebra. The cranial margin, however, does not grow proportional with the vertebral column, and thus it “descends” from the level of the fifth thoracic vertebra in CS16 to the

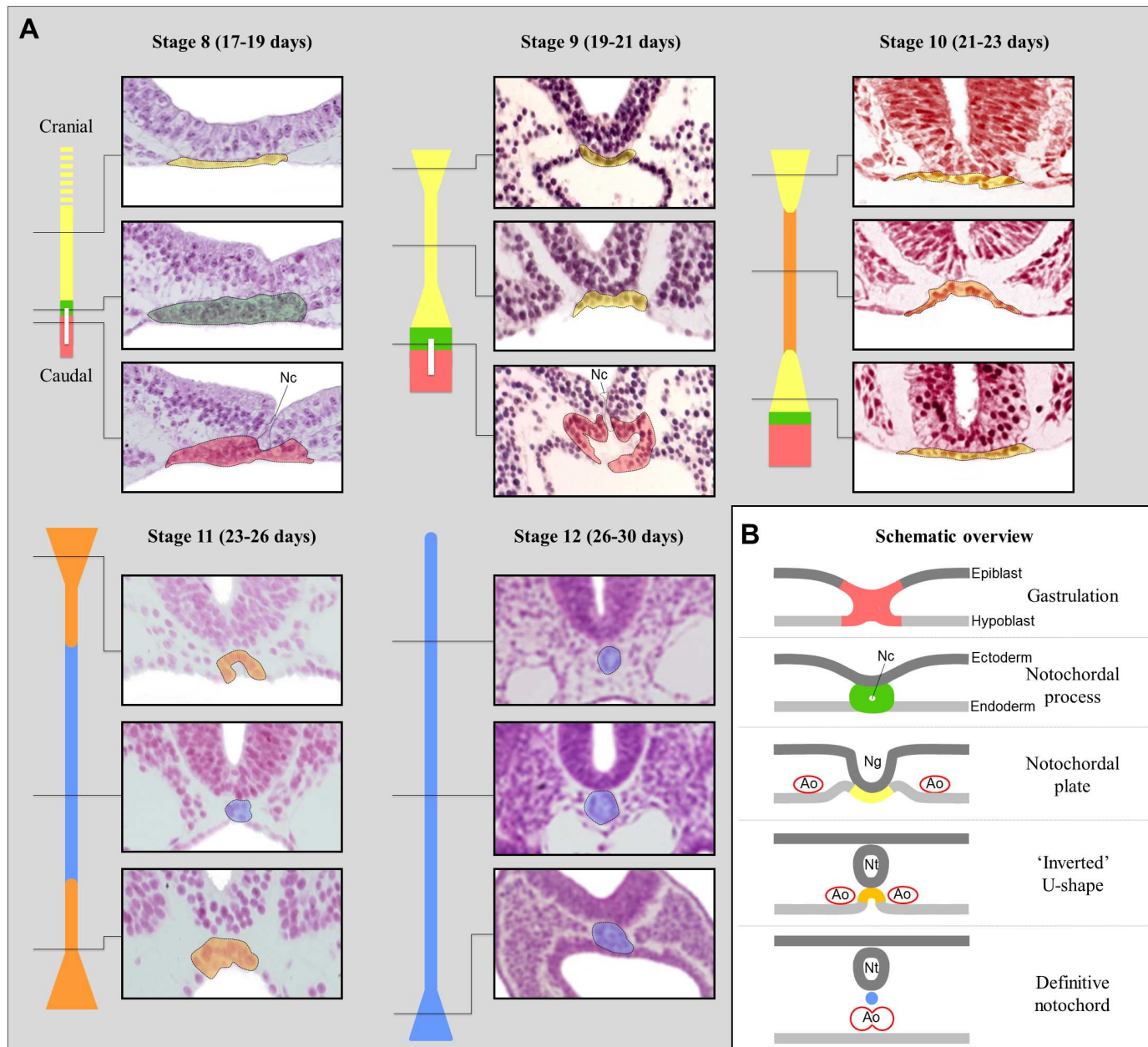


Fig. 6. Schematic overview of the development of the notochord.

(A) The notochord develops from stages 8 to 12. Three representative transverse sections per stage are shown along with a schematic representation of the developing notochord, showing the position of the sections and the partitions of the developing notochord. The notochordal process and plate develop in craniocaudal direction, whereas formation of the definitive notochord starts in the middle of the embryo, expanding in both directions. The caudal extreme of

the developing notochord widens in stage 12 (26 to 30 days) as a result of secondary development in the caudal eminence. (B) Schematic overview of the five stages of notochordal development in a transverse view. Red, gastrulation zone; green, notochordal process with notochordal canal; yellow, notochordal plate; orange, “inverted U”-shaped notochord; blue, definitive notochord; Ao, aorta; Nc, neureneric canal; Ng, neural groove; Nt, neural tube. Presented specimens are 10175, 3709, 6330, 6344, and 8505A.

second lumbar vertebra in CS23 (Fig. 5). Obviously, this does not imply that the gonad, as an organ, truly descends in this period, but merely that it shortens relative to the growing vertebrae. Analysis of 34 specimens of the first 2 months of human development thus enabled us to elicit the information required to describe the changes in the position of internal organs relative to one another (data S2).

Comparative morphological analyses

In the absence of human experimental studies, medical embryologists necessarily rely heavily on data obtained from experimental animals such as chicken and mouse. A proper understanding of the development of birth defects thus requires insight into the similarities and differences between human development and that of these experimental animals. However, it is not clear whether car-

toons of certain developmental processes in medical textbooks truly reflect the human situation. The data collected for the current atlas remedy this situation because they allow verification of experimental findings in the developing human. We cite two examples.

The first example is the development of the notochord, represented in textbooks as a mixture of human and animal data (4, 5, 37). Figure 6

shows the human sections of the relevant developmental stages in our atlas, along with cartoons indicating our observations. These data show that in humans, a group of primitive cells briefly persists after gastrulation. This transient group of cells, through which the neureneric canal traverses, is dubbed the notochordal process. The ventral side of this cell cluster is incorporated into the endodermal roof of the foregut, and its dorsal side is closely attached to the developing neural tube. This intimate association is often ignored, even though animal studies have shown that the developing notochord induces the formation of the floor plate of the neural tube (38) and is attached to the developing neural system (39, 40). Then the notochordal process incorporates entirely into the endoderm, forming the epithelial notochordal plate, which adopts an “inverted U” shape and remains intimately associated with the neural tube. Subsequently, the notochordal cells detach from the endoderm to form the definitive notochord, allowing the two dorsal aortas to fuse between the notochord and the roof of the foregut (Fig. 6B). Similar to gastrulation, the formation of the notochordal process and plate proceeds in the craniocaudal direction. However, in contrast to the mechanism described in several textbooks (3–6), the formation of the definitive notochord in humans starts in the middle of the embryo and then proceeds in both cranial and caudal directions, similar to what is generally assumed for the closure of the neural tube.

The second example relates to the origin of the derivatives of the pharyngeal arches. According to current theories, the hyoid body develops by fusion of parts of the second and third pharyngeal arch cartilages, and the thyroid cartilage by fusion of parts of the fourth and sixth pharyngeal arch cartilages, as described for lower vertebrates (41). In contrast, we observed that in human development, the body of the hyoid bone develops from a single growth center, without overt contributions from the second and third pharyngeal arch cartilages. The thyroid and cricoid cartilages develop separately from mesenchymal thickenings (fig. S4). Anatomical variations of the hyoid-larynx complex occur in up to 25% of the general population (42). Most variants are not important in the clinical setting, but they may be important in a forensic context if a fracture of the hyoid bone is suspected. In that case, it is of utmost importance to distinguish between true fractures of the hyoid bone or the thyroid horns, and failure of these parts to fuse during development.

Discussion

The recent expansion of molecular genetic technology has brought with it an improved understanding of the regulatory mechanisms that control the development of the vertebrate building plan. Although the findings in model organisms are being extrapolated to human development, insight into the divergence and conservation of human morphogenesis, as compared to experimental animals, remains crucial to assess whether such extrapolations are justified. A global analy-

sis of the changing position of just a few structures such as the gonads, kidneys, and arteries shows discrepancies with current textbooks and thus demonstrates the value of a 3D atlas based on human embryonic specimens. The generated 3D models are presented in interactive 3D-PDF files (43), which facilitates the understanding of complex 3D structures and permits the reader to develop an independent judgment about human embryology. Although new editions of biomedical textbooks update recent molecular insights, the morphogenesis is not updated and has become increasingly schematic as well as alienated from the original human substrate. This 3D atlas reinstates this link because the morphological reconstructions are connected directly to the original sections of the human embryos in the Carnegie Collection.

Our atlas can serve as an educational and reference resource for (bio)medical students, clinicians, and scientists interested in human development and development-related disease. The original images and reconstructions are available for educational use and further scientific analysis. This, in turn, will permit updates and extension of the atlas with time, in cooperation with other research groups.

REFERENCES AND NOTES

- “Congenital anomalies,” WHO Fact sheet No370 (2014).
- “Birth Defects,” WHO Executive board 125th session EB125/7 (2009).
- B. M. Carlson, *Human Embryology and Developmental Biology* (Elsevier Saunders, ed. 5, 2014).
- K. L. Moore, T. V. N. Persaud, M. G. Torchia, *The Developing Human: Clinically Oriented Embryology* (Elsevier, ed. 10, 2016).
- T. W. Sadler, *Langman’s Medical Embryology* (Wolters Kluwer Health, ed. 13, 2015).
- G. C. Schoenwolf, S. B. Bleyl, P. R. Brauer, P. H. Francis-West, *Larsen’s Human Embryology* (Elsevier Saunders, ed. 5, 2015).
- I. Broman, *Die Entwicklung des Menschen vor der Geburt* (J. F. Bergmann, München, 1927).
- M. Foster, F. M. Balfour, *The Elements of Embryology* (Macmillan, 1874).
- R. F. Gasser, *Atlas of Human Embryos* (Harper & Row, 1975).
- C. H. Heuser, A presomite human embryo with a definite chorda canal. *Contrib. Embryol.* **23**, 251–267 (1932).
- C. H. Heuser, J. Rock, A. T. Hertig, Two human embryos showing early stages of the definitive yolk sac. *Contrib. Embryol.* **31**, 85–99 (1945).
- W. His, *Anatomie Menschlicher Embryonen vol. I* (Vogel, Leipzig, 1880).
- W. His, *Anatomie Menschlicher Embryonen vol. II* (Vogel, Leipzig, 1882).
- W. His, *Anatomie Menschlicher Embryonen vol. III* (Vogel, Leipzig, 1885).
- F. Keibel, F. P. Mall, *Manual of Human Embryology. Volume I* (Lippincott, 1910).
- F. Keibel, F. P. Mall, *Manual of Human Embryology. Volume II* (Lippincott, 1912).
- A. Keith, *Human Embryology and Morphology* (William Wood, Baltimore, 1933).
- R. O’Rahilly, F. Müller, *Developmental Stages in Human Embryos* (Carnegie Institution, 1987).
- C. W. Prentiss, L. B. Arey, *A Laboratory Manual and Text-Book of Embryology* (Saunders, 1917).
- G. L. Streeter, Developmental horizons in human embryos. Description of age group XI, 13 to 20 somites, and age group XII, 21 to 29 somites. *Contrib. Embryol. Carnegie Inst.* **30**, 211–245 (1942).
- G. L. Streeter, Developmental horizons in human embryos. Description of age group XIII, embryos about 4 or 5 millimeters long, and age group XIV, period of indentation of the lens vesicle. *Contrib. Embryol. Carnegie Inst.* **31**, 27–63 (1945).
- G. L. Streeter, Developmental horizons in human embryos. Description of age groups XV, XVI, XVII, and XVIII, being the third issue of a survey of the Carnegie collection. *Contrib. Embryol. Carnegie Inst.* **32**, 133–203 (1948).
- G. L. Streeter, Developmental horizons in human embryos; a review of the histogenesis of cartilage and bone. *Contrib. Embryol. Carnegie Inst.* **33**, 149–168 (1949). pmid: 1814445
- G. L. Streeter, Developmental horizons in human embryos. Description of age groups XIX, XX, XXI, and XXII, being the fifth issue of a survey of the Carnegie Collection. *Contrib. Embryol. Carnegie Inst.* **34**, 165–196 (1951).
- Y. Matsuda et al., Super-parallel MR microscope. *Magn. Reson. Med.* **50**, 183–189 (2003). doi: 10.1002/mrm.10515; pmid: 12815693
- S. Yamada, T. Nakashima, A. Hirose, A. Yoneyama, T. Takeda, T. Takakuwa, in *The Human Embryo*, S. Yamada, T. Takakuwa, Eds. (InTech, Rijeka, 2012), chapter 7.
- Federative International Programme on Anatomical Terminologies (FIPAT), *Terminologia Embryologica, International Embryological Terminology* (Georg Thieme Verlag, 2013).
- S. F. Gilbert, *Developmental Biology* (Sinauer Associates, ed. 9, 2010).
- W. J. Hamilton, J. D. Boyd, H. W. Mossman, *Human Embryology. Prenatal Development of Form and Function* (Heffers, Cambridge, 1972).
- H. Tuchmann-Duplessis, P. Haegel, *Illustrated Human Embryology, Vol.2 Organogenesis* (Springer-Verlag, 1974).
- H. Butler, B. H. Juurlink, *An Atlas for Staging Mammalian and Chick Embryos* (CRC Press, 1987).
- R. O’Rahilly, D. B. Meyer, The timing and sequence of events in the development of the human vertebral column during the embryonic period proper. *Anat. Embryol.* **157**, 167–176 (1979). doi: 10.1007/BF00305157; pmid: 517765
- N. J. Sissman, Developmental landmarks in cardiac morphogenesis: Comparative chronology. *Am. J. Cardiol.* **25**, 141–148 (1970). doi: 10.1016/0002-9149(70)90575-8; pmid: 5413193
- W. J. Larsen, *Human Embryology* (Churchill Livingstone, New York, 1993).
- W. S. Costa, F. J. Sampayo, L. A. Favorito, L. E. Cardoso, Testicular migration: Remodeling of connective tissue and muscle cells in human gubernaculum testis. *J. Urol.* **167**, 2171–2176 (2002). doi: 10.1016/S0022-5347(05)65122-1; pmid: 11956474
- F. Müller, R. O’Rahilly, The initial appearance of the cranial nerves and related neuronal migration in staged human embryos. *Cells Tissues Organs* **193**, 215–238 (2011). doi: 10.1159/000320026; pmid: 20980719
- H. Tuchmann-Duplessis, G. David, P. Haegel, *Illustrated Human Embryology. Vol. 1: Embryogenesis* (Springer-Verlag, 1982).
- H. W. M. Straaten, J. W. M. Hekking, E. J. L. M. Wiertz-Hoessels, F. Thors, J. Drukker, Effect of the notochord on the differentiation of a floor plate area in the neural tube of the chick embryo. *Anat. Embryol.* **177**, 317–324 (1988). doi: 10.1007/BF00315839; pmid: 3354847
- A. Jurand, The development of the notochord in chick embryos. *J. Embryol. Exp. Morphol.* **10**, 602–621 (1962). pmid: 13958100
- A. Jurand, Some aspects of the development of the notochord in mouse embryos. *J. Embryol. Exp. Morphol.* **32**, 1–33 (1974). pmid: 4141719
- A. S. Romer, *The Vertebrate Body* (Saunders, 1962).
- P. J. de Santana Júnior et al., Which is your diagnosis? *Radiol. Bras.* **42**(4), 11–12 (2009); www.rbr.org.br/detalhe_artigo.asp?id=987. doi: 10.1590/0100-3984.2014.47.5qd; pmid: 25741099
- J. Muriene, A. Ziegler, B. Ruthensteiner, A 3D revolution in communicating science. *Nature* **453**, 450 (2008). doi: 10.1038/453450d; pmid: 18497796

ACKNOWLEDGMENTS

We thank R. J. Cork and R. F. Gasser of the Virtual Human Embryo project (<http://virtualhumanembryo.lsuhsc.edu>) for kindly providing the photographs of the first series of sections of human embryos of the Carnegie Collection; E. Lockett and E. Wilson of the National Museum of Health and Medicine (Silver Spring, Maryland) for providing access to the Carnegie Collection; G. Burton for generously providing the digital images of a stage

9 embryo of the Boyd Collection, scanned by A. Shelley; O. J. G. B. de Bakker and B. Meijer for their assistance in photographing the sections; K. Aben, Z. Al-Shabani, C. Berends, H. Boon, F. Bounif, C. Buijs, M. Buijtenendijk, D. M. de Bakker, K. de Cuba, B. de Jong, J. de Jong, S. Dekker, I. de Vries, M. de Witte, I. El-Bouyahaoui, M. Ghariq, E. Groot, C. Hafkamp, N. Hagemeyer, I. Harmsen, L. Hassing, D. Henssen, E. Hodde, D. Hoornstra, B. Hulstein, J. Kruiderier, L. Kuil, T. Lachkar, S. Levy, R. Linschoten, J. Maarleveld, R. Michael, F. Noyola, M. Oppelaar, R. Post, G. Roelandt, M. Seinen, M. Slooter, D. Smidt, F. Stubenruch, D. Torenstra, O. Turgman, S. van Wieringen,

H. van Willigen, M. van der Poel, J. van Genderen, B. Verhoef, M. Warmbrunn, and S. Zomer for annotation of the sections; A. Linnenbank, B. Bakker, P. de Weert, J. Gieskens, G. Lens, J. Kalle, Y. Kim, R. Moolenaar, R. Pesch, J. Pouw, R. Rana, P. Stroombergen, D. van Etten, and P. van der Linden for modeling the structures; and R. H. Anderson and B. A. de Boer for scientific support and critical reading of the manuscript. The atlas content (3D-PDFs, source images, and labeled images in TIFF and AMIRA format) can be downloaded from <http://3datlasofhumanembryology.com>. Chicken and mouse sections are available from the corresponding authors.

SUPPLEMENTARY MATERIALS

www.sciencemag.org/content/354/6315/aag0053/suppl/DC1
Materials and Methods
Supplementary Text
Figs. S1 to S4
Tables S1 to S3
Data S1 to S3
Supplementary 3D-PDFs (14 Files, Stages 7 to 23)
References (44–51)

29 April 2016; accepted 11 October 2016
10.1126/science.aag0053

EXTENDED PDF FORMAT
SPONSORED BY



An interactive three-dimensional digital atlas and quantitative database of human development

Bernadette S. de Bakker, Kees H. de Jong, Jaco Hagoort, Karel de Bree, Clara T. Besselink, Froukje E. C. de Kanter, Tyas Veldhuis, Babette Bais, Reggie Schildmeijer, Jan M. Ruijter, Roelof-Jan Oostra, Vincent M. Christoffels and Antoon F. M. Moorman (November 24, 2016)

Science **354** (6315), . [doi: 10.1126/science.aag0053]

Editor's Summary

Digital reconstruction of human development

The detailed morphology of human development has intrigued scientists and the medical field alike. However, the scarcity of specimens hampers detailed mapping of tissue architecture. Furthermore, inaccuracies in the description of human development have crept into textbooks from observations of animal models that are extrapolated to humans. By mapping normal developmental processes and patterns, such as the growth and relative placement of organs, congenital anomalies can be better understood. de Bakker *et al.* generated interactive three-dimensional digital reconstructions based on the Carnegie collection of histologically sectioned human embryos spanning the first 2 months of gestation. These interactive models will serve as educational and scientific resources for normal and abnormal human development.

Science, this issue p. 10.1126/science.aag0053

This copy is for your personal, non-commercial use only.

Article Tools

Visit the online version of this article to access the personalization and article tools:

<http://science.sciencemag.org/content/354/6315/aag0053>

Permissions

Obtain information about reproducing this article:

<http://www.sciencemag.org/about/permissions.dtl>

Science (print ISSN 0036-8075; online ISSN 1095-9203) is published weekly, except the last week in December, by the American Association for the Advancement of Science, 1200 New York Avenue NW, Washington, DC 20005. Copyright 2016 by the American Association for the Advancement of Science; all rights reserved. The title *Science* is a registered trademark of AAAS.